Journal Pre-proofs

Accumulation of 2-Acetylamino-5-mercapto-1,3,4-thiadiazole in chitosan coatings for improved anticorrosive effect on zinc

Árpád Ferenc Szőke, Gabriella Stefánia Szabó, Zoltán Hórvölgyi, Emőke Albert, Attila Gergely Végh, László Zimányi, Liana Maria Muresan

PII: S0141-8130(19)34555-6
DOI: https://doi.org/10.1016/j.ijbiomac.2019.09.114
Reference: BIOMAC 13359

To appear in:

Received Date: 18 June 2019
Revised Date: 2 September 2019
Accepted Date: 15 September 2019

Please cite this article as: A. Ferenc Szőke, G. Stefánia Szabó, Z. Hórvölgyi, E. Albert, A. Gergely Végh, L. Zimányi, L. Maria Muresan, Accumulation of 2-Acetylamino-5-mercapto-1,3,4-thiadiazole in chitosan coatings for improved anticorrosive effect on zinc, (2019), doi: https://doi.org/10.1016/j.ijbiomac.2019.09.114

This is a PDF file of an article that has undergone enhancements after acceptance, such as the addition of a cover page and metadata, and formatting for readability, but it is not yet the definitive version of record. This version will undergo additional copyediting, typesetting and review before it is published in its final form, but we are providing this version to give early visibility of the article. Please note that, during the production process, errors may be discovered which could affect the content, and all legal disclaimers that apply to the journal pertain.

Journal Pre-proofs

Accumulation of 2-Acetylamino-5-mercapto-1,3,4-thiadiazole in chitosan coatings for improved anticorrosive effect on zinc

Árpád Ferenc Szőke[a1], Gabriella Stefánia Szabó[a2], Zoltán Hórvölgyi[b], Emőke Albert[b], Attila Gergely Végh[c], László Zimányi[c], Liana Maria Muresan[a1*]

[a]*Babeş-Bolyai University, Faculty of Chemistry and Chemical Engineering, Research Center in Electrochemistry and Non-conventional Materials,* [1]*Department of Chemical Engineering,* [2]*Department of Chemistry and Chemical Engineering of the Hungarian Line, Romania, RO-400028, Cluj-Napoca, 11 Arany János St.*

E-mail: limur@chem.ubbcluj.ro

[b]*Budapest University of Technology and Economics, Faculty of Chemical Technology and Biotechnology, Department of Physical Chemistry and Materials Science, Centre for Colloid Chemistry, Hungary, HU-1111, Budapest, Budafoki út 6-8.*

[c]*Institute of Biophysics, Biological Research Centre, Hungarian Academy of Sciences, Hungary H-6726, Szeged, Temesvári Krt. 62.*

Declarations of interest: none.

Abstract

Chitosan (Chit) coatings were applied on zinc substrates by the dip-coating method. Subsequently, the coatings were impregnated with a corrosion inhibitor, 2-Acetylamino-5-mercapto-1,3,4-thiadiazole (AcAMT) to obtain an increased anticorrosive effect. The coating thickness and the AcAMT accumulation were determined using UV-Vis spectroscopy on glass and quartz substrates, respectively. The surface morphology and coverage were investigated with atomic force microscopy. Electrochemical impedance spectroscopy and potentiodynamic polarization techniques were used to investigate the protective properties of the impregnated coatings. The chitosan coatings facilitated the accumulation of the corrosion inhibitor inside the polymeric matrix (a multiplication of 380 times compared to the impregnating solution concentration was calculated), channeling high amounts of AcAMT to the Zn surface, which resulted in an inhibition efficiency of >90%. This effect demonstrates the applicability of chitosan coatings as carriers for corrosion inhibitors, significantly reducing the amount of inhibitor needed to achieve good anticorrosive effects.

Keywords: chitosan; zinc corrosion; 2-acetylamino-5-mercapto-1,3,4-thiadiazole.

Journal Pre-proofs

1. Introduction

Chitosan is a linear polysaccharide composed of randomly distributed β-(1-4)-linked D-glucosamine and N-acetyl-D-glucosamine [1], produced by the deacetylation of chitin obtained from natural sources. Due to its environmentally friendly nature, the relatively simple and low-cost manufacturing process [2], the high availability of the raw material, as well as its solubility in acidic media through protonation of its amine groups [3], chitosan has attracted significant attention in recent years. On account of its versatility, chitosan is utilized in numerous fields of application, including the production of nanoparticles and thin films [4, 5].

Dip-coating has proven to be a highly efficient method to produce chitosan coatings with well-controlled characteristics on various substrates [6], however, the low barrier properties of native chitosan coatings [7, 8] can limit their application in anticorrosive protection. Modification of chitosan by ionic or covalent crosslinking has had mixed results regarding anticorrosive protection [6, 9], with the reduced flexibility of crosslinked chitosan often being an issue [10, 11]. An alternative approach can be to take advantage of the gel-form matrix and the positive charge of the protonated chitosan chains (Figure 1 A and Figure 1s B – supplementary data), which make the material an efficient adsorbent for negatively charged molecules [12, 13, 14]. A further advantage of chitosan-coating is the transparency of the layers, providing protection without modifying the visual aspect of the coated object [15].

2-Acetylamino-5-mercapto-1,3,4-thiadiazole (AMT) is a non-toxic [16] organic molecule. AcAMT and similar compounds are currently studied as possible diuretics, antimicrobial and anticancer agents [17, 18]. Another application of AcAMT is its use as a corrosion inhibitor. Sulfur and nitrogen-containing molecules are preferentially adsorbed on metals [19], hindering the access of corrosive species to the metal surface. AcAMT was previously reported as an efficient corrosion inhibitor for copper and bronze [20], 2-amino-5-mercapto-1,3,4-thiadiazole

was used in the protection of mild steel [19], while other thiadiazoles and sulfur-containing molecules were successfully applied in the protection of bronze [21] and zinc [22]. Nevertheless, to the extent of our knowledge, no studies were reported on the anticorrosive properties of AcAMT on zinc.

It is common knowledge that in neutral and slightly acidic conditions, a certain amount of AcAMT is negatively charged (Figure 1 B, Figure 1s – supplementary data) [23]. This generates the possibility of its accumulation in positively charged chitosan through ionic forces (including hydrogen bond formation) from such impregnating solutions.

In this context, the present study aims to gain a high anticorrosive effect by accumulating AcAMT in the gel matrix of chitosan layers applied on zinc substrates. These novel coatings have the advantage of easy removability without damaging the underlying zinc surface, granting them high effectiveness in the temporary protection of zinc during transport [5, 14, 24].

The extent of inhibitor accumulation was determined on glass and quartz substrates by UV-Vis spectroscopy. Raman spectroscopy studies demonstrated the formation of the chitosan layer on the Zn substrate and the presence of AcAMT within the chitosan layer. The protective properties of the films were investigated by electrochemical impedance spectroscopy (EIS) and potentiodynamic polarization methods. The coating coverage and changes of the surface morphology during the corrosion process were studied with atomic force microscopy (AFM), and showed increased protection during prolonged corrosive exposure when the chitosan layer was infiltrated by AcAMT.

2. Materials and Methods

2.1. Reagents

Zinc plates were acquired from Bronzker Bt. and cut into samples of 2 × 5 cm. Menzel-Gläser microscope glass slides and Suprasil 1 quartz slides were purchased from Thermo Scientific and Optilab Kft., respectively.

99% Na_2SO_4 from Merck was used to prepare the electrolyte solution. 99.8% acetic acid and isopropanol were provided by Lachner. WF-flex-16 abrasive paper was purchased from Hermes, while the micropolish alumina powder (with a particle size of 0.3 μm) was from Buehler. Medium molecular weight chitosan was acquired from Aldrich (viscosity: 200-800 cP for 1w/w % in 1% acetic acid solution). Deionized water 18.2 MΩ·cm, purified with Millipore Simplicity 185 filtration system was used to prepare all solutions. Pure AcAMT was acquired from Aldrich.

All chemicals were of analytical grade and used without any purification step.

2.2.Substrate preparation and coating

Prior to coating, the glass and quartz substrates were cleaned successively by an aqueous detergent solution, 10% V/V H_2SO_4, isopropanol, distilled water and deionized water. Zinc plates were prepared for coating by polishing with abrasive papers with different roughness (P1200, P2000, P2500) and the 0.3 μm particle size Al_2O_3. Between each step, the plates were washed with distilled water. Finally, any residue from the polishing process was removed from the zinc surface with two rounds of ultrasonication in isopropanol for 5 minutes. Any left-over zinc oxide was cleaned by dipping the layers for 5 seconds in 0.1 M HCl solution [5].

A 1 w/w% aqueous chitosan solution was prepared by dissolving the appropriate amounts of chitosan powder in 1 w/w% aqueous acetic acid solution [25]. The mixture was left overnight

for the chitosan dissolution to take place. Due to the deacetylation degree of chitosan greatly affecting solubility [26], any insoluble chitosan residue (due to incomplete deacetylation) was removed by a 30-minute centrifugation step at 4000 rpm.

The polished and cleaned zinc, glass and quartz samples were coated from the 1 w/w% chitosan solution, using the dip-coating technique (dip-coater, Plósz Mérnökiroda Kft., Hungary) at a constant immersion and withdrawal speed of 5 cm/min. The temperature of the chitosan solution was maintained constant at 25°C. The coated samples were left to dry for 24 hours at room temperature.

During the coating and drying process, the samples were protected from any dust, which can be a source of inhomogeneity.

For inhibitor impregnation, the dried samples were immersed with a speed of 1 cm/min into a 1 mM aqueous solution of AcAMT for 15 minutes, before being withdrawn and rinsed with distilled water [5].

2.3.UV-Vis and Raman spectroscopy

The coating thickness, refractive index, AcAMT accumulation and leaching from the chitosan matrix were investigated using UV-Vis spectroscopy.

The transmittance spectra of the bare and coated glass substrates were recorded at 350-1100 nm wavelength range with a 10 nm/s scanning speed and 1 nm resolution on an Analytic Jena Specord 200-0318 spectrophotometer.

Transmittance spectra of the samples were analyzed in terms of thin-layer optical models. The spectra recorded on glass substrates were fitted with a homogeneous layer model which is based on optical admittance [27]. The model supposes a perpendicular angle of incidence, as well as identical, homogeneous, isotropic and flat layers on both sides of the transparent substrate

[27]. The fitting procedures provided layer thickness and effective refractive index (at 632.8 nm) values. The glass substrates had weak absorption, therefore, in order to eliminate the effect, the transmittance spectra of the chitosan samples were corrected with the absorption of their substrates before fitting [27, 28]. For the fitting procedure, the Levenberg – Marquardt algorithm was used [29].

In order to ascertain the inhibitor accumulation, the absorbance spectra of the chitosan-coated and AcAMT impregnated chitosan-coated quartz samples were recorded with a 10 nm/s scanning speed and 1 nm resolution at 190-500 nm wavelength range. Due to the weak absorbance of the unimpregnated, chitosan-coated quartz, the recorded spectra were corrected to determine the absorbance attributable to AcAMT.

The approximate accumulation of the inhibitor was determined by using the molar absorptivity of AcAMT for aqueous solutions [5].

Raman spectroscopy was used to demonstrate the presence of AcAMT inside the chitosan coatings applied on Zn substrates. The Raman spectra of uncoated zinc, chitosan-coated zinc and Zn/Chit-AcAMT were recorded with an Ntegra Spectra, NT-MDT Spectrum Instruments Raman microscope, under air at ambient temperature in the range of 484 to 1952 cm^{-1}. A 25 x 10 μm area was studied for Zn and 24 x 30 μm areas for Zn/Chit and Zn/Chit-AcAMT, respectively with a step size of 0.5 μm in both directions of the studied plane. A single spectrum was assigned to each system by averaging all recorded spectra in the studied area. In order to obtain the spectra attributed to the native and impregnated chitosan coatings, features characteristic of Zn were canceled out by subtracting the bare Zn spectrum multiplied by a wavenumber dependent linear weighing function.

2.4.Atomic force microscopy

Atomic force microscopy images were recorded for Zn/Chit and Zn/Chit-AcAMT samples before and after 3 days of exposure to a 0.2 g/L Na_2SO_4 corrosive solution.

High-resolution topographies were recorded with an MFP-3D atomic force microscope, (Asylum Research, Santa Barbara CA; driving software written in IgorPro 6.34A, Wavemetrics). Rectangular silicon cantilevers with a tetrahedral tip with a radius below 10 nm were used in these measurements (AC240, Olympus, Optical Co. Ltd. Tokyo, Japan). Prior to measurements, the spring constant for each cantilever was calibrated, according to standard built-in procedures [30, 31], prior to measurements. The images were recorded with a typical resolution of 512 by 512 pixels, with a scan speed of 10 µm/s in a closed loop. In order to correct potential sample tilt, all height images were first-order flattened and planefitted.

2.5. Electrochemical investigation

In order to determine the anticorrosive effect of each sample, an electrochemical study was carried out on a PARSTAT-2273 single-channel potentiostat (Princeton Applied Research, United States) in an undivided electrochemical cell containing the zinc samples (active surface area = 2 cm^2) as the working electrode, a platinum wire as the counter (Type P131 Radiometer, France) and a Ag/AgCl, KCl_{sat} reference electrode (Radiometer, France). All experiments were carried out at room temperature (25 ± 1°C).

2.5.1. Electrochemical impedance spectroscopy (EIS)

EIS measurements were carried out in a frequency interval of 10^{-2} Hz - 10^4 Hz, with a potential amplitude of 10 mV, at open circuit potential (OCP) in 0.2 g/L aqueous Na_2SO_4 solution (pH = 5) to determine the effect of short and long term exposure of the samples to a corrosive

solution. Chitosan-coated samples were either kept continuously in the electrolyte solution during the 4 days of the study (while recording their EIS spectra each day); or were only immersed in the corrosive environment shortly before recording their impedance spectra, dried afterward and kept in air between measurement, forced to repeat swelling-drying cycles.

Equivalent circuits were fitted to the experimental data by using ZSimpWin 3.21 from EChem software.

2.5.2. Polarization studies

Both linear (at low overpotentials - OCP ± 20 mV) and semilogarithmic (at high overpotentials - OCP ± 200 mV) polarization curves were recorded to determine the kinetic parameters and to ascertain the anticorrosive properties of the inhibitor and the coatings. Polarization curves were recorded with a scan rate of 10 mV/min and were interpreted with the aid of Electrochemistry PowerSuite v2.56, provided by the manufacturer. Corrosion current densities (i_{corr}) were determined using the Stern-Geary equation [32]:

$$i_{corr} = \frac{b_a \cdot b_c}{2.3Rp \cdot (b_a + b_c)}, \quad (1)$$

where b_a and b_c are the Tafel slopes determined from the semilogarithmic polarization curves and Rp is the polarization resistance determined from the Nyquist impedance diagrams.

For uncoated Zn and Zn/Chit, the low slope of the polarization curves in the cathodic branch points to a diffusion-controlled process. In diffusion-controlled cases, $b_c \rightarrow \infty$, and a simplified version of the Stern-Geary equation was applied to determine the corrosion current densities [33]:

$$i_{corr} = \frac{1}{2.303Rp\left(\frac{1}{ba} + \frac{1}{|bc|}\right)} = \frac{b_a}{2.303Rp} \quad (2)$$

The inhibition efficiency of each system was determined using the following equation:

$$IE(\%) = 100 \cdot \frac{i^0_{corr} - i_{corr}}{i^0_{corr}}, \quad (3)$$

where i^0_{corr} is the value of the corrosion current density of the bare Zn sample, while i_{corr} is the corrosion current density of coated systems.

Given that polarization studies only reflect the behavior of the exposed metal surface (in our case the spots where open pseudo-pores are present in the chitosan coating), and presuming that the chitosan coatings are electrochemically inert at low overpotentials [34], a pseudo-porosity can be calculated using the following equation [35]:

$$P = \frac{Rp_s}{Rp} \cdot 10^{-(\Delta E_{corr}/b_a)} \cdot 100\ (\%), \quad (4)$$

where P is the pseudo-porosity of the protective layer, Rp_s is the polarization resistance of the metal, Rp is the polarization resistance of the coated Zn, ΔE_{corr} is the difference between the corrosion potentials of the bare zinc and the coated metal (from the linear polarization measurements), and b_a is the anodic Tafel coefficient for the substrate.

3. Results and discussion

3.1.Optical characterization

The refractive index and thickness of the chitosan coating were determined using a thin layer optical model [27] from 6 chitosan-coated glass samples (Figure 2s – supplementary data). The determined mean refractive index of 1.5382 ± 0.0008 and mean layer thickness of 404 ± 9 nm showed only small deviations, pointing to a good reproducibility of the coating.

After impregnation, the absorbance spectra of the samples showed a strong absorbance peak at 319 nm (suggesting the accumulation of the inhibitor). Additionally, a slight shift compared to the absorbance maximum of AcAMT in aqueous solution (313 nm) was observed.

Using the molar absorptivity coefficient determined from the aqueous solutions (ε = 16.14 $cm^{-1}\mu M^{-1}$, Figure 2 A), the concentration of AcAMT impregnated into the chitosan matrix was approximated. Results show a significant concentration-multiplication, compared to the impregnating solution, of 379 ± 13. It is assumed that AcAMT molecules enter the pores of the chitosan coating, reaching the metal surface, where they are adsorbed and exert an inhibiting effect.

The successful incorporation of AcAMT was also demonstrated by Raman spectroscopy measurements, where multiple peaks appeared (684, 967, 1080, 1119, 1259, 1383, 1463, 1554, 1682 cm^{-1}) on the AcAMT impregnated chitosan. These peaks can only be attributed to the presence of AcAMT in the chitosan coating (Figure 2 B), as peaks with similar positions could also be observed in the Raman spectrum for pure AcAMT powder. Comparing the peak positions between AcAMT powder and impregnated AcAMT, some shifts can be observed, due to the chitosan matrix affecting the vibrations of the inhibitor molecule. The strong signal from the presence of AcAMT mostly overlaps that of the native chitosan.

3.2.Morpho-structural analysis before and after corrosion

Upon visual inspection (Figure 3s – supplementary data), no cracking or peeling of the coatings was observed before or after impregnation, despite conflicting results reported previously on the adhesion between chitosan and metal substrates [5, 36, 37]. Significant damage (peeling or cracking) to the coatings was only observed after long term immersion of the samples in the aqueous Na_2SO_4 solution (t > 3 days) and only in the vicinity of pre-existing metal defects.

Journal Pre-proofs

This effect is more prominent in the case of native Chit coatings. A possible explanation for this good adhesion is the presence of trace amounts of zinc hydroxide and oxide on the substrate surface which can greatly improve adhesion [36].

Atomic force microscopy measurements

The effectiveness of the coating process was verified with atomic force microscopy.

AFM images and height profiles show a homogenous coverage for both chitosan and AcAMT-impregnated chitosan coatings (Figure 3). The low surface roughness, which reaches a maximum at around 100 nm is significantly less than the layer thickness determined with UV-Vis spectroscopy (*ca.* 400 nm). This suggests a good coverage of the zinc substrates, protecting them from direct exposure to corrosive environments.

After 3 days in a corrosive solution (Figure 4), the AcAMT impregnated samples retained their structural integrity. Native chitosan coatings, however, show notable signs of degradation with a highly increased surface roughness and even holes on the surface of the coating (Figure 4 C).

Even if AcAMT cannot have a significant effect on the permeability of the chitosan coatings (ionic crosslinking cannot occur under the studied conditions due to it requiring multiple negative charges on the impregnating molecule), it protects the underlying zinc substrate, also preventing damage to the coating.

3.3.Electrochemical study

3.3.1. Polarization curves

The linear and semilogarithmic polarization curves of all studied samples are presented in Figure 5 and the data obtained are summarized in Table 1.

The interpretation of polarization curves should take into consideration that the complex process of corrosion of the coated samples includes the swelling of the coatings by electrolyte/water intake, and even a possible adsorption/deposition of corrosion products on the coating surface. In addition, we need to take into consideration the fact that the Tafel curves reflect only the electrochemical activity of the exposed zinc surface, where the electrolyte permeates through the pseudo-pores of the chitosan coating, gaining access to the metal. In view of the above, determining electrochemical characteristics of the coated zinc samples is not completely rigorous with either AC or DC methods [5, 38], but even so, the interpretation of the polarization curves can provide valuable information on the anticorrosive properties of coated systems [5, 39].

3.3.1.1. Inhibition efficiency of studied systems

The polarization resistance values of each system determined from EIS or linear polarization are in good agreement. Measurements done at both low and high overpotentials show similar results for bare Zn, bare Zn measured in the presence of 10^{-3}M AcAMT solution, and chitosan-coated Zn, suggesting relatively weak corrosion resistance of these samples. On the contrary, impregnating the chitosan coatings with AcAMT has a significant anticorrosive effect, observed by the slope-hindering of the linear polarization curves and the decrease of the corrosion current densities of the semilogarithmic curves. Upon interpretation with the Stern-Geary method, these initial observations were confirmed. The relatively low anticorrosive effect calculated for native chitosan coatings (IE = 64%) was attributed to the high permeability of the coatings, while the IE of 75% observed in the presence of the 10^{-3}M AcAMT solution points to an insufficient concentration of inhibitor near the metal substrate for effective protection. Using the chitosan coatings to drive an increased amount of AcAMT through the pseudo-pores towards the metal surface increased the inhibition efficiency to 91%.

3.3.1.2. Effect of impregnation on the corrosion potential and pseudo-porosity of chitosan

The corrosion potential of the Zn/Chit-AcAMT system shows a positive shift of 79 mV compared to that of bare Zn suggesting an ennoblement of the metal.

The pseudo-porosity (*calculated with equation (4)*) of the coated samples (after 1 hour of OCP) was significantly lower (8%) than that of the native chitosan coatings (42%), suggesting that AcAMT has sealed the majority of the pores after adsorption on the metallic surface where it acted as a corrosion inhibitor.

3.3.2. Electrochemical impedance spectroscopy

To determine the corrosion rate for coated metals, an AC technique such as EIS has been proven to be more subtle than the DC technique of Tafel plotting. The Nyquist impedance diagrams for Zn, Zn/AcAMT, Zn/Chit and Zn/Chit-AcAMT systems are presented in Figure 6. All diagrams appear as depressed semi-circles, while a distinctive inductive loop was also observed for both chitosan-coated systems. It can be seen that after impregnation with AcAMT, the coating's polarization resistance increased significantly. This is in good agreement with the data obtained from the polarization curves.

The changes that occur to the coated systems over time were monitored by recording the impedance spectra during several days and by identifying the corresponding equivalent circuits (Figure 7). The suitability of the fitting was verified through the Chi^2 values that were around 10^{-3} or lower in all cases; the results are presented in Table 2.

3.3.2.1. EIS study of Zn/Chit systems

Journal Pre-proofs

For the Zn/Chit system, initially, an $R(Q_1R_1(LR_2))$ equivalent electrical circuit gave the best fitting, with R representing the resistance of the electrolyte solution. R_1 was attributed to the charge transfer resistance at the interface between the underlying zinc substrate and the electrolyte solution entering the chitosan matrix during the constant swelling of the polymer. The capacitance of the electric double layer was substituted with a Q_1 constant phase element (due to the non-ideal behavior of the studied systems). The inductive portion of the impedance curves was attributed to the chitosan coatings' behavior during the swelling process [5, 40]. Thus, the behavior of chitosan is represented in the equivalent circuit by an LR_2 series, connected in parallel with the elements corresponding to the electron transfer on the zinc-electrolyte interface. It can be observed that, while being kept in the electrolyte solution, the corrosion resistance of the coated samples gradually decreased due to the increased permeability and degradation of the coatings. With the swelling of the chitosan reaching its end, the equivalent circuit is reduced to $R(Q_1R_1)$ after 1 day of immersion.

3.3.2.2. EIS study of Zn/Chit-AcAMT systems

For the impregnated Zn/Chit-AcAMT system, similar results were obtained, but the initial R_1 resistance was significantly higher (7.78 $k\Omega cm^2$) than in the case of native chitosan (2.05 $k\Omega cm^2$). Previous studies concluded that low amounts of a crosslinking agent cannot have a significant effect on the properties of chitosan coatings [5]. As only a small percentage of AcAMT has a negative charge at the studied parameters (pH = 5), we can conclude that AcAMT cannot have a significant crosslinking effect on the chitosan coatings. Thus, the increase in resistance points to significant accumulation of AcAMT in the chitosan coating ensuring an enhanced access of AcAMT to the metal surface, resulting in an increased protection efficiency. As in the case of the native chitosan coatings, the equivalent circuit was reduced to $R(Q_1R_1)$ after 1 day of immersion.

These results point to a good initial effect of the inhibitor that is diminished when exposed to the corrosive solution for a prolonged period of time. This is due to the leaching of AcAMT from the chitosan coatings in parallel with Na_2SO_4 diffusion into the polymer layer, which makes a corrosive attack possible.

Zn/Chit-AcAMT samples were also tested by removing them from the electrolyte solution after recording their impedance spectra and keeping them in air between measurements. This exposes the coatings to swelling-drying cycles, which could damage them significantly. However, during intermittent measurements over a period of 4 days, no damage was observed to the coatings and the anticorrosive resistance was preserved to a greater extent than in the case of the samples kept constantly in Na_2SO_4 (Figure 8). Swelling-drying cycles can induce degradation of the chitosan layer by producing cracks in the coating. The fact that the impregnated chitosan coating can be exposed to multiple swelling-drying cycles while retaining most of its resistance points to the retained flexibility and durability of the chitosan layer.

4. Conclusions

Chitosan coatings were applied to zinc substrates with the dip-coating method in an effort to enhance the anticorrosive effects 2-Acetylamino-5-mercapto-1,3,4-thiadiazole. The coating thickness and the AcAMT accumulation were studied by UV-Vis spectroscopy on coated glass and quartz substrates. The surface of the zinc samples before and after corrosion was analyzed by AFM. The anticorrosive effect of the coatings was investigated by electrochemical methods.

AFM results showed a low surface roughness (*ca*. 100 nm) compared to the coating thickness (*ca.* 400 nm) and a good surface coverage from both the native Chit and the

Journal Pre-proofs

impregnated Chit-AcAMT coatings. The Zn/Chit samples showed notable signs of degradation, while the Zn/Chit-AcAMT samples retained their structural integrity even after 3 days of exposure to a corrosive environment.

Polarization studies proved a synergistic effect of AcAMT and chitosan, with the polymer coating channeling increased amounts (accumulation of *ca.* 380 times compared to the impregnating solution) of inhibitor to the zinc surface, resulting in an inhibition efficiency of >90%.

Impedance spectroscopy studies showed a good initial effect from AcAMT impregnation, which becomes weaker at prolonged exposures to corrosive media. The stability of the coatings was considerably higher when they were kept in air and only exposed to the corrosive environment during intermittent measurements.

Due to their non-toxic nature, and low requirement for raw material, Chit-AcAMT coatings can be successfully used in the temporary protection of zinc objects that require further processing at a later date. Once swollen, chitosan coatings are easily removable without damaging the metal substrate.

Such coatings can also serve as good model systems to study the accumulation of negatively charged molecules inside a polymer matrix and the permeability of thin polymer films.

Acknowledgments

Árpád Szőke is grateful for the financial support provided by the Romanian Ministry of National Education, the WFS and KMEI associations. In addition, he wishes to thank Dr. Balázs Szalontai for helping in the Raman measurement and Zsuzsanna Márton. This work was supported by the Collegium Talentum 2018 Programme of Hungary. The research reported in this

Journal Pre-proofs

paper was supported by the Higher Education Excellence Program of the Ministry of Human Capacities in the frame of Nanotechnology and Materials Science research area of Budapest University of Technology and Economics (BME FIKP-NAT). The research work has been accomplished in the framework of the "BME R+D+I project", supported by the grant TÁMOP 4.2.1/B-09/1/KMR-2010-0002. An NRDI TNN-123631 grant and an NRDI K-128266 grant are acknowledged. Emőke Albert's research work was supported by the European Union and the State of Hungary, co-financed by the European Social Fund in the framework of TÁMOP-4.2.4.A/2-11/1-2012-0001 "National Excellence Program". The support by the Economic Development and Innovation Operational Programme, Hungary [grant number GINOP 2.3.2-15-2016-00001] is also acknowledged.

The data that support the findings of this study are available from the corresponding author, [L. M.], upon reasonable request.

References

1. M.E. Morales, M.A. Ruiz, Microencapsulation of probiotic cells: applications in nutraceutic and food industry, in: A.M. Grumezescu (Eds.), Nanotechnology in the Agri-Food Industry, Nutraceuticals, Academic Press, 2016, pp. 627-668. https://doi.org/10.1016/B978-0-12-804305-9.00016-6.
2. R.C. Cheung, T.B. Ng, J.H. Wong, W.Y. Chan, Chitosan: An Update on Potential Biomedical and Pharmaceutical Applications, Mar. drugs 13(8) (2015) 5156-5186. https://doi.org/10.3390/md13085156.
3. M. Rinaudo, Properties and degradation of selected polysaccharides: hyaluronan and chitosan, Corros. Eng. Sci. Techn. 42(4) (2007) 324-334.

https://doi.org/10.1179/174327807X238945.

4. A. Abdelgawad, S. Hudson, Chitosan nanoparticles: Polyphosphates cross-linking and protein delivery properties, Int. J. Biol. Macromol. (2019). https://doi.org/10.1016/j.ijbiomac.2019.06.062.
5. Á.F. Szőke, G.S. Szabó, Z. Hórvölgyi, E. Albert, L. Gaina, L.M. Muresan, Eco-friendly indigo carmine-loaded chitosan coatings for improved anti-corrosion protection of zinc substrates, Carbohyd. Polym. 215 (2019) 63-72. https://doi.org/10.1016/j.carbpol.2019.03.077.
6. L.Y. Pozzo, T.F. Conceição, A. Spinelli, N. Scharnagl, A.T.N. Pires, Chitosan coatings crosslinked with genipin for corrosion protection of AZ31 magnesium alloy sheets, Carbohyd. Polym. 181 (2018) 71–77. http://dx.doi.org/10.1016/j.carbpol.2017.10.055.
7. D.R. Rohindra, A.V. Nand, J.R. Khurma, Swelling properties of chitosan hydrogels, SPJNS 22 (2004) 32-35. https://doi.org/10.1071/SP04005.
8. D. Nataraj, S. Sakkara, M. Meghwal, N. Reddy, Crosslinked chitosan films with controllable properties for commercial applications, Int. J. Biol. Macromol. 120(A) (2018) 1256-1264. https://doi.org/10.1016/j.ijbiomac.2018.08.187.
9. J. Carneiro, J. Tedim, M.G.S. Ferreira, Chitosan as a smart coating for corrosion protection of aluminum alloy 2024: A review, Prog. Org. Coat. 89 (2015) 348-356. https://doi.org/10.1016/j.porgcoat.2015.03.008.
10. T. Jóźwiak, U. Filipkowska, P. Szymczyk, J. Rodziewicz, A. Mielcarek, Effect of ionic and covalent crosslinking agents on properties of chitosan beads and sorption effectiveness of Reactive Black 5 dye, React. Funct. Polym. 114 (2017) 58-74. https://doi.org/10.1016/j.reactfunctpolym.2017.03.007.

11. J. Khouri, A. Penlidis, Viscoelastic properties of crosslinked chitosan films, Processes 7(157) (2019) 1-18. https://doi.org/10.3390/pr7030157.
12. D. Liudvinaviciute, K. Almonaityte, R. Rutkaite, J. Bendoraitiene, R. Klimaviciute, Adsorption of rosmarinic acid from aqueous solution on chitosan powder, Int. J. Biol. Macromol. 118(A) (2018) 1013-1020. https://doi.org/10.1016/j.ijbiomac.2018.06.166.
13. S.-K. Kim, Chitin, Chitosan, Oligosaccharides and Their Derivates, 1st ed., CRC Press, Boca Raton, 2010. https://doi.org/10.1201/EBK1439816035.
14. J. Carneiro, J. Tedim, S.C.M. Fernandes, C. Freire, A. Gandini, M. Ferreira, M.L. Zheludkevich, Chitosan as a Smart Coating for Controlled Release of Corrosion Inhibitor 2-Mercaptobenzothiazole, ECS Electrochem. Lett. 2 (2013) 19-22. http://doi.org/10.1149/2.002306eel.
15. S.C.M. Fernandes, C.S.R. Freire, A.J.D. Silvestre, C.P. Neto, A. Gandini, L.A. Berglund, L. Salmén, Transparent chitosan films reinforced with a high content of nanofibrillated cellulose, Carbohyd. Polym. 81(2) (2010) 394-401. https://doi.org/10.1016/j.carbpol.2010.02.037.
16. United Stated Environmental Protection Agency. 2019 (accessed 6th June 2019) https://comptox.epa.gov/dashboard/dsstoxdb/results?search=DTXSID00186535#exec_sum
17. I. Matysiak, Biological and Pharmacological Activities of 1,3,4-Thiadizaole Based Compounds, Mini-Rev. Med. Chem. 15(9) (2015) 762-775. http://doi.org/10.2174/1389557515666150519104057.

18. G.L. Almajan, A. Innocenti, L. Puccetti, G. Manole, S. Barbuceanu, I. Saramet, A. Scozzafava, C.T. Supuran, Carbonic anhydrase inhibitors. Inhibition of the cytosolic and tumor-associated carbonic anhydrase isozymes I, II, and IX with a series of 1,3,4-thiadiazole- and 1,2,4-triazole-thiols, Bioorg. Med.Chem. Lett. 15(9) (2005) 2347-2352. https://doi.org/10.1016/j.bmcl.2005.02.088.
19. R. Solmaz, G. Kardaş, G. Kardaş, B. Yazici, B. Yazici, M. Erbil, Adsorption and corrosion inhibitive properties of 2-amino-5-mercapto-1,3,4-thiadiazole on mild steel in hydrochloric acid media, Colloid. Surf. A Physicochem. Eng. Asp. 312(1) (2008) 7-17. http://doi.org/10.1016/j.colsurfa.2007.06.035.
20. J. Chelaru, L. Muresan, 2-mercapto-5-acetylamino-1,3,4-thiadiazole as corrosion inhibitor for a naturally patinated monumental bronze artifact, Studia UBB Chemia 59 (2014) 91-102.
21. S. Varvara, L.M. Muresan, K. Rahmouni, H. Takenouti, Evaluation of some non-toxic thiadiazole derivatives as bronze corrosion inhibitors in aqueous solution, Corros. Sci. 50(9) (2008) 2596-2604. https://doi.org/10.1016/j.corsci.2008.06.046.
22. R.L. Leroy, Chelate Inhibitors for Zinc and Galvanized Products, Corrosion, 34(3) (1978) 98-109. http://doi.org/10.5006/0010-9312-34.3.98.
23. Instant Cheminformatics Solutions, http://www.chemicalize.com. 2019 (accessed 6th June 2019)
24. Á.F. Szőke, G. Szabó, Z. Simó, Z. Hórvölgyi, E. Albert, A.G. Végh, L. Zimányi, L.M. Muresan, Chitosan coatings ionically cross-linked with ammonium paratungstate as anticorrosive coatings for zinc, Eur. Polym. J. 118 (2019) 205-212.

Journal Pre-proofs

https://doi.org/10.1016/j.eurpolymj.2019.05.057.

25. M. Dabóczi, E. Albert, E. Agócs, M. Kabai-Faix, Z. Hórvölgyi, Bilayered (silica-chitosan) coatings for studying dye release in aqueous media: The role of chitosan properties, Carbohyd. Polym. 136 (2016) 137-145. https://doi.org/10.1016/j.carbpol.2015.09.025.
26. C. Wang, F. Yuan, J. Pan, S. Jiao, L. Jin, H. Cai, A novel method for the determination of the degree of deacetylation of chitosan by coulometric titration, Int. J. Biol. Macromol. 70 (204) 306-311. https://doi.org/10.1016/j.ijbiomac.2014.07.007.
27. E. Hild, A. Deák, L. Naszályi, Ö. Sepsi, N. Ábrahám, Z. Hórvölgyi, Use of the optical admittance function to simulate and evaluate transmittance spectra of graded-index colloidal films, J. Opt. A-Pure Appl. Opt. 9 (2007) 920-930. https://doi.org/10.1088/1464-4258/9/10/023.
28. D.S. Hinczewski, M. Hinczewski, F.Z. Tepehan, G.G. Tepehan, Optical filters from SiO_2 and TiO_2 multi-layers using sol-gel spin coating method, Sol. Energ. Mat. S. C. 87 (2005) 181-196. https://doi.org/10.1016/j.solmat.2004.07.022.
29. W.H. Press, B.P. Flannery, S.A. Teukolsky, W.T. Vetterling, Numerical Recipes in C, The Art of Scientific Computing, Cambridge University Press, New York, 1988.
30. J.L. Hutter, J. Bechhoefer, Calibration of atomic-force microscope tips, Rev. Sci. Instrum. 64(7) (1993) 1868–1873. https://doi.org/10.1063/1.1143970.
31. J.E. Sader, J.A. Sanelli; B.D. Adamson, J.P. Monty, X. Wei, S.A. Crawford, J.R. Friend, I. Marusic, P. Mulvaney, E.J. Bieske, Rev. Sci. Instrum. 83(10) (2012) 103705.

Journal Pre-proofs

https://doi.org/10.1063/1.4757398.

32. K. Kanno, M. Suzuki, Y. Sato, Tafel slope determination of corrosion reaction by the coulostatic method, Corros. Sci. 20(8-9) (1980) 1059-1066. https://doi.org/10.1016/0010-938X(80)90084-0.
33. E. McCafferty, in Introduction to corrosion science, 1st ed., Springer (2010), 159-162. http://dx.doi.org/ 10.1007/978-1-4419-0455-3.
34. R. A. Zangmeister, J. J. Park, G. W. Rubloff, M. J. Tarlov, Electrochemical study of chitosan films deposited from solution at reducing potentials, Electrochim. Acta 51(25) (2006) 5324–5333. http://doi.org/10.1016/j.electacta.2006.02.003.
35. B. Elsener, A. Rota, H. Böhni, Impedance study on the corrosion of PVD and CVD titanium nitride coatings, Mater. Sci. Forum 44-45 (1989) 29-38. http://doi.org/10.4028/www.scientific.net/msf.44-45.29.
36. O. Lundvall, M. Gulppi, M.A. Paez, E. Gonzalez, J.H. Zagal, J. Pavez, G.E. Thompson, Copper modified chitosan for protection of AA-2024, Surf. Coat. Tech. 201(12) (2007) 5973-5978. https://doi.org/10.1016/j.surfcoat.2006.11.005.
37. C. Fernández-Solis, A. Erbe, Waterborne chitosan-epoxysilane hybrid pretreatments for corrosion protection of zinc, Biointerphases, 11(2) (2016):021001, 1-10 https://doi.org/10.1116/1.4944828.
38. S. Feliu, J.M. Bastidas, J.C. Galvan, S. Feliu Jr., J. Simancas, M. Morcillo, E. Almeida, Electrochemical determination of rusted steel surface stability, J. Appl. Electrochem. 23 (1993) 157-161. http://dx.doi.org/doi:10.1007/bf00246953.

Journal Pre-proofs

39. J. Balaji, M.G. Sethuraman, Chitosan-doped-hybrid/TiO2 nanocomposite based sol-gel coating for the corrosion resistance of aluminum metal in 3.5% NaCl medium, Int. J. Biol. Macromol. 104(B) (2017) 1730-1739. https://doi.org/10.1016/j.ijbiomac.2017.03.115.

40. B.P. Setzler, T.F. Fuller, A Physics-Based Impedance Model of Proton Exchange Membrane Fuel Cells Exhibiting Low-Frequency Inductive Loops, J. Electroanal. Chem. 162(6) (2015) 519-530.
https://doi.org/10.1149/2.0361506jes.

Journal Pre-proofs

FIGURE CAPTIONS

Figure 1. Molecular structure of protonated chitosan (**A**) and the deprotonation of the AcAMT molecule with the increase of pH (**B**)

(Also see Figure 1s A and B – supplementary data)

Figure 2 A: Calibration curves for AcAMT determined from aqueous solution with UV-Vis spectroscopy at 319 nm. Absorbance spectra of 50 μM AcAMT (inset) in an aqueous solution (continuous black line) and in an impregnated chitosan coating (dashed black line).

B: Raman spectra of pure AcAMT powder, Zn, Chit and Chit-AcAMT after adjustments determined from coated zinc samples.

Figure 3. AFM images (A, A1, B, B1) and height profiles (A2, B2) of the surface of Zn/Chit (A, A1, A2) and Zn/Chit-AcAMT (B, B1, B2) systems before corrosion

Figure 4. AFM images (C, C1, D, D1) and height profiles (C2, D2) of the surface of Zn/Chit (C, C1, C2) and Zn/Chit-AcAMT (D, D1, D2) systems after 3 days of corrosion in a 0.2 g/L aqueous Na_2SO_4 solution.

Some deposited crystals can be noticed on the surface, probably from Na_2SO_4 that has entered the chitosan matrix during swelling.

Figure 5: Linear (A) and semi-logarithmic (B) polarization curves of Zn (●), Zn/AcAMT solution (Δ), Zn/Chit (○) and Zn/Chit-AcAMT (▲) samples; Experimental conditions: 0.2 g/L aqueous Na_2SO_4 solution (pH =5), scan rate, 0.166 mV/s, OCP, 60 minutes.

Figure 6: Nyquist impedance spectra of Zn (●), Zn/AcAMT solution (Δ), Zn/Chit (○) and Zn/Chit-AcAMT (▲) systems. Experimental conditions: 0.2 g/L aqueous Na_2SO_4 solution, (pH =5), frequency interval, 10 mHz - 10kHz, OCP, 60 minutes, amplitude, 10 mV

Figure 7: **A**: Nyquist impedance spectra of Zn/Chit after different immersion times

B: Nyquist impedance spectra of Zn/Chit-AcAMT after different immersion times

I, II: Fitted equivalent circuits

Immersion times: 1 hour - ●; 1 day - ○; 2 days - ●; 3 days - ▲; 4 days - Δ; all equivalent circuit fittings are noted with black lines.

Experimental conditions: 0.2 g/L Na_2SO_4 solution, frequency interval, 10 mHz - 10kHz, OCP 60 minutes, amplitude, 10 mV

Figure 8: Nyquist impedance spectra of Zn/Chit-AcAMT system held in air between measurements, over a period of 4 days. Experimental conditions: 0.2 g/L aqueous Na_2SO_4 solution (pH = 5), frequencies, 10 mHz - 10 kHz, OCP, 60 minutes (day 0), 10 minutes (days 1-4), amplitude, 10 mV

Journal Pre-proofs

FIGURES

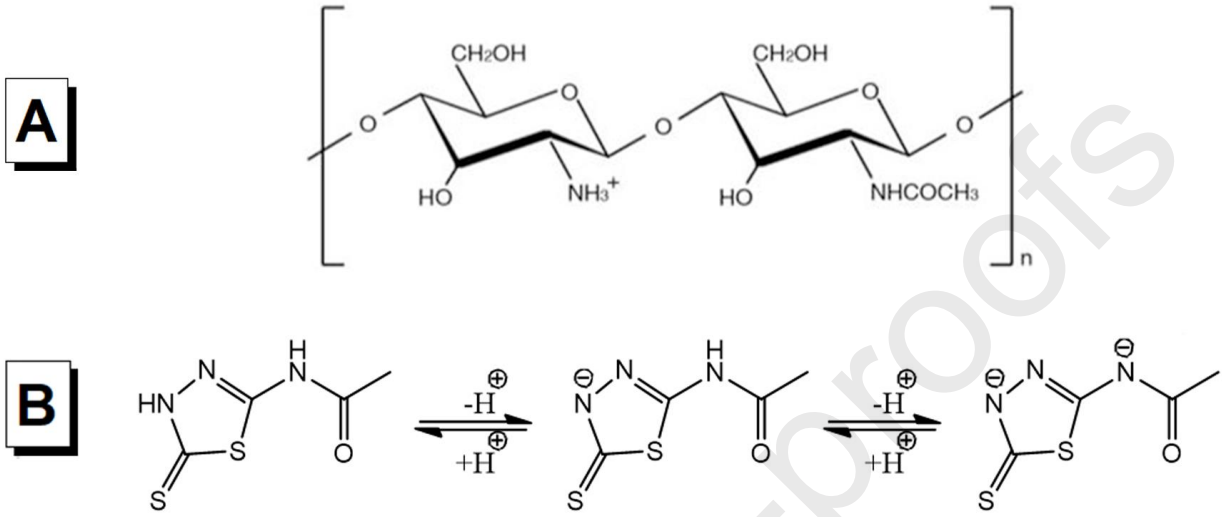

Figure 1

Journal Pre-proofs

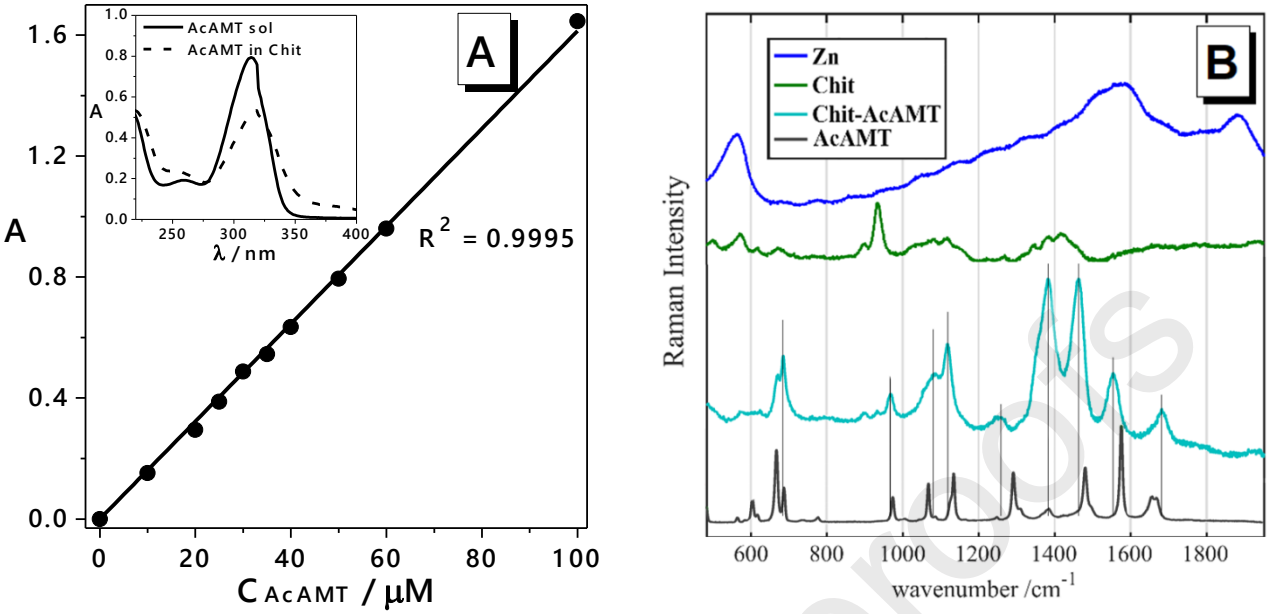

Figure 2

Journal Pre-proofs

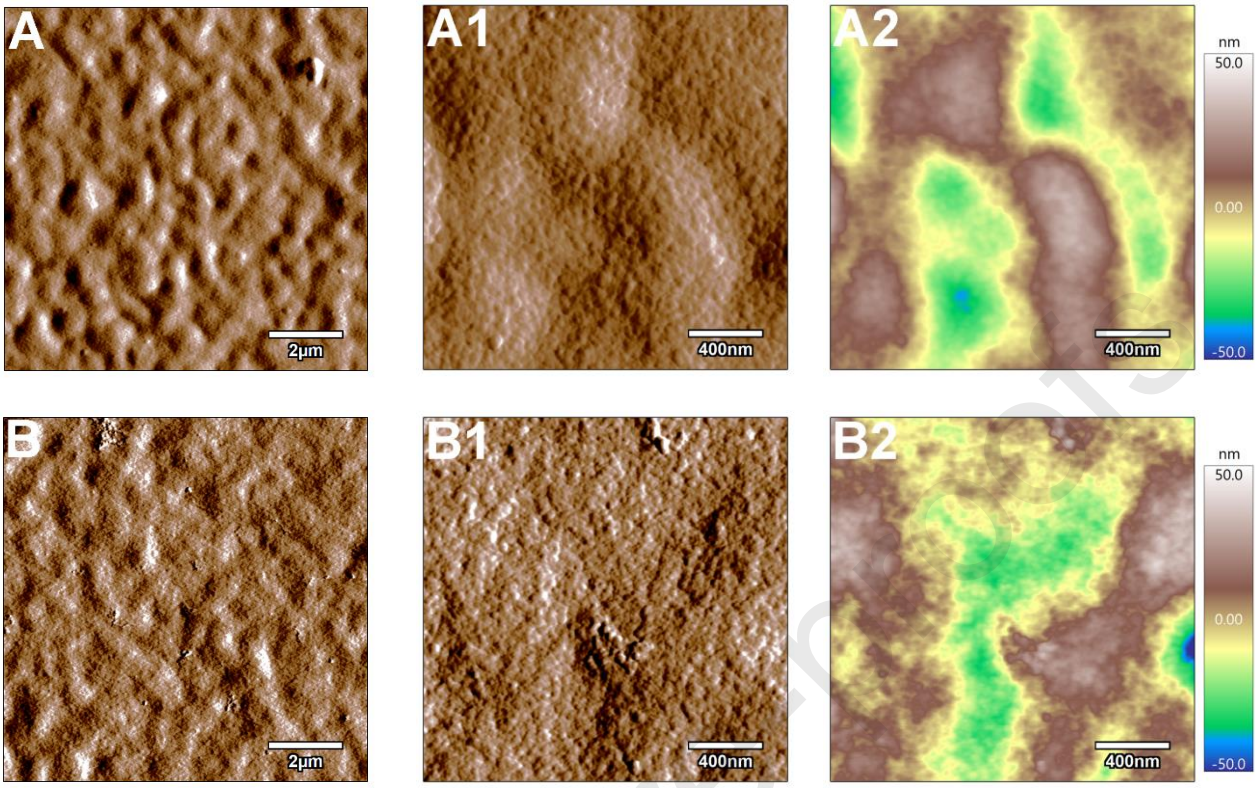

Figure 3

Journal Pre-proofs

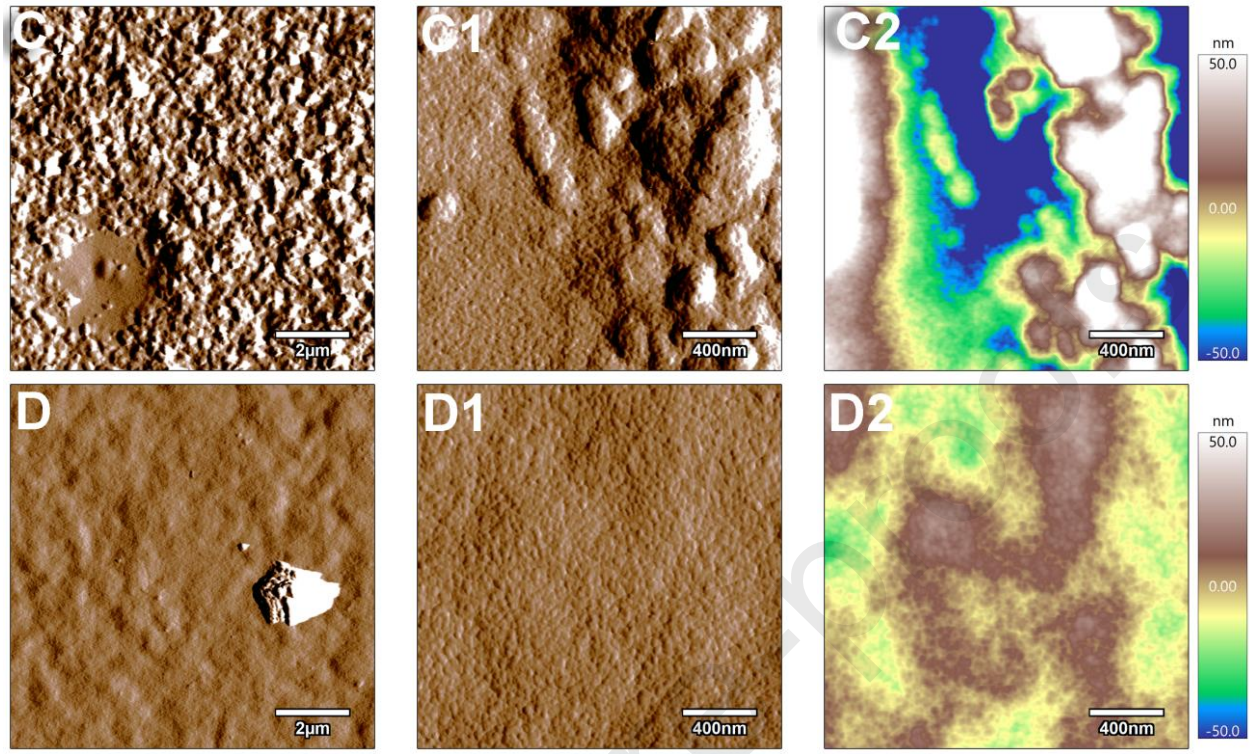

Figure 4

Journal Pre-proofs

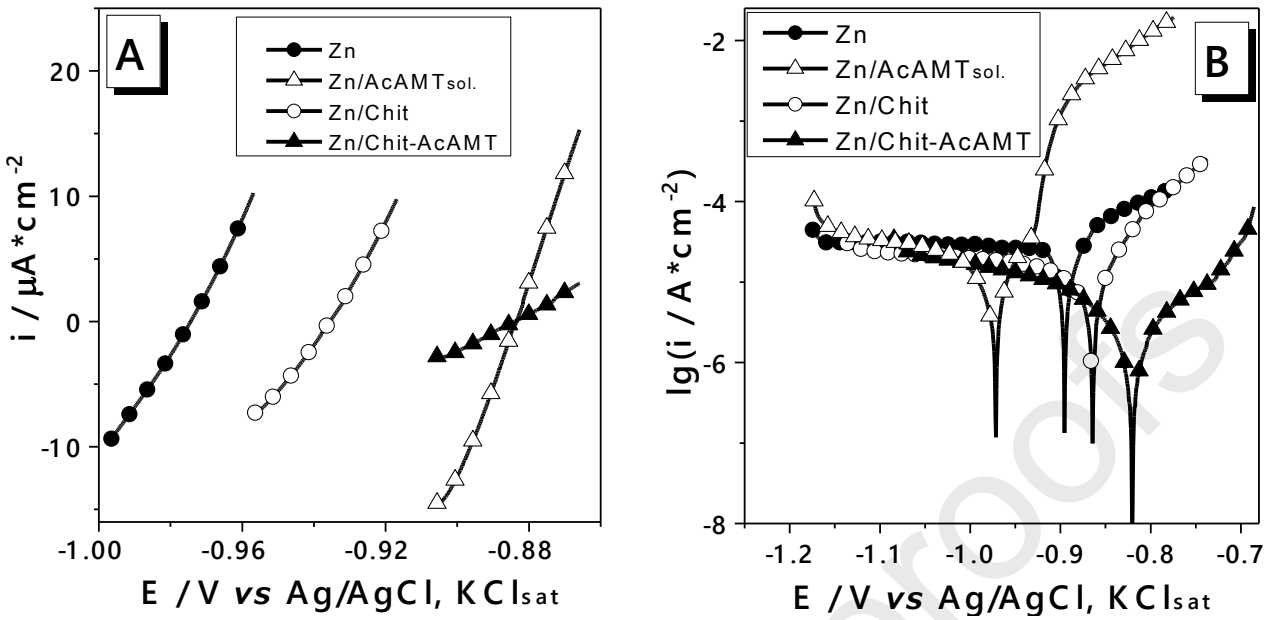

Figure 5

Journal Pre-proofs

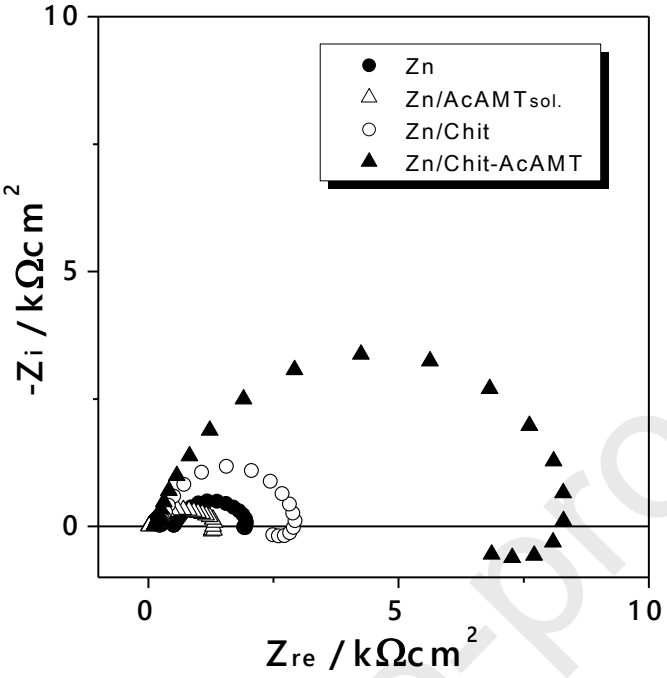

Figure 6

Journal Pre-proofs

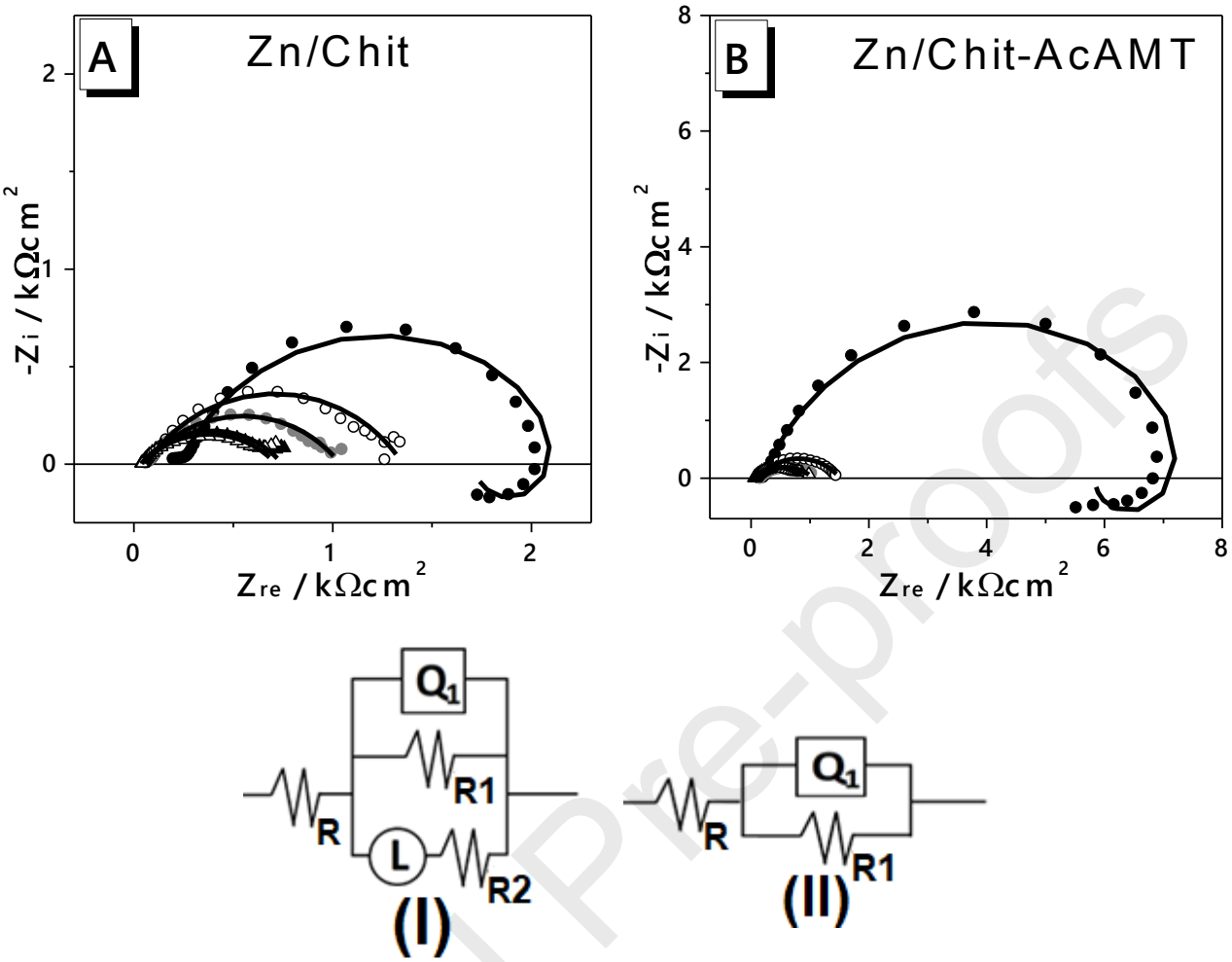

Figure 7

Journal Pre-proofs

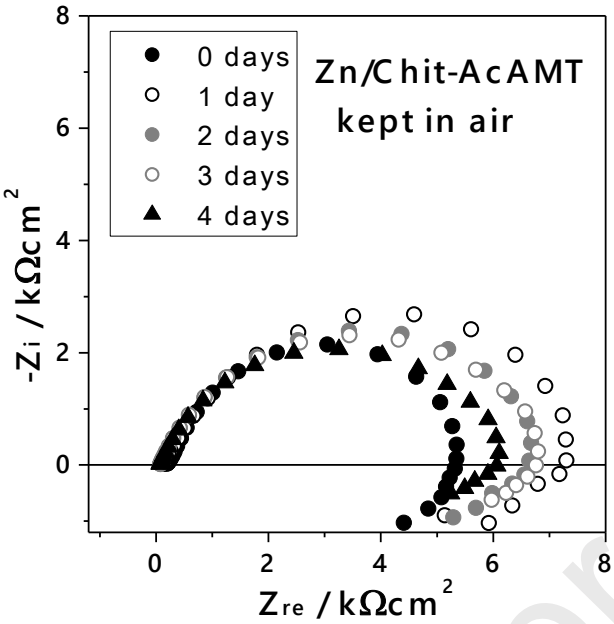

Figure 8

Journal Pre-proofs

TABLES

Table 1. Corrosion parameters for various coated zinc samples determined with the Stern-Geary equation

Sample	E_{corr} (V vs RE) (lin. pol)	E_{corr} (V vs RE)	b_c (V/dec)	b_a (V/dec)	i_{corr} (μA / cm^2)	Rp (Ωcm^2) (lin.pol)	R_p (Ωcm^2) (EIS)	IE (%)
Zn	-0.975	-0.896	-	0.195	43.56	2002	1944	-
Zn/AcAMT sol.	-0.975	-0.971	0.303	0.038	11.08	1151	1325	74.56
Zn/Chit	-0.936	-0.865	-	0.105	15.56	2315	2929	64.28
Zn/Chit-AcAMT	-0.884	-0.817	0.151	0.137	3.77	6676	8290	91.35

Journal Pre-proofs

Table 2. Parameter values for Zn/Chit and Zn/Chit-AcAMT coated samples calculated by non-linear regression of the impedance data using the equivalent electrical circuits from Figure 7

Immersion time	R (kΩcm^2)	R_1 (kΩcm^2)	Q_1 (μSs^n)	L (kH)	R_2 (kΩcm^2)	Chi^2
			Zn/Chit			
1 hour	0.231	2.05	108.40	27.33	5.50	7.62×10^{-3}
1	0.065	1.29	226.90	-	-	6.82×10^{-3}
2	0.059	0.98	297.40	-	-	1.86×10^{-3}
3	0.036	0.71	398.10	-	-	1.41×10^{-3}
4	0.040	0.68	493.40	-	-	1.71×10^{-3}
			Zn/Chit-AcAMT			
1 hour	0.208	7.78	22.67	50.22	20.58	4.27×10^{-3}
1	0.116	1.40	250.60	-	-	9.27×10^{-4}
2	0.139	0.91	467.20	-	-	5.60×10^{-4}
3	0.050	0.82	462.20	-	-	1.39×10^{-3}
4	0.067	0.84	530.60	-	-	2.31×10^{-3}

Journal Pre-proofs

APPENDICES

-supplementary material-

Abbreviations and symbols used	
OCP	open circuit potential
i, i_{corr}	current density and corrosion current density
E, E_{corr}	potential and corrosion potential
b_c, b_a	cathodic and anodic Tafel coefficient
RP	polarization resistance
IE	inhibition efficiency
Z_i	imaginary part of the complex impedance
Z_{re}	real part of the complex impedance
R	resistance
Q	electric charge
L	electric inductance
AFM	atomic force microscopy
Chit	chitosan
AcAMT	2-Acetylamino-5-mercapto-1,3,4-thiadiazole

Journal Pre-proofs

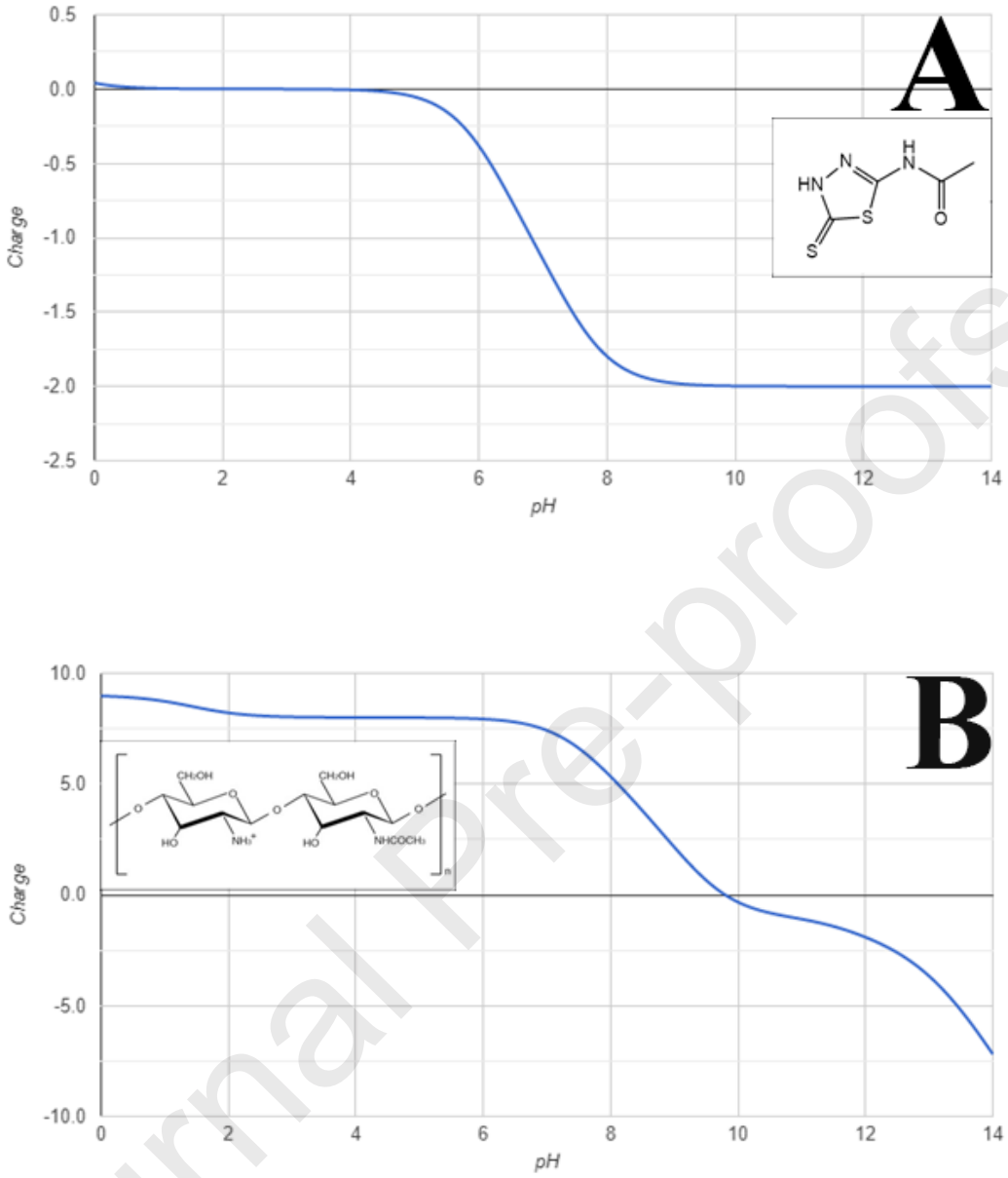

Figure 1s: pH dependence of the charge of 2-Acetylamino-5-mercapto-1,3,4-thiadiazole (A) and a chitosan molecule with a molar mass of 1526.46 g/mol (B)

Source: chemicalize.com, accessed on 06.06.2019.

Journal Pre-proofs

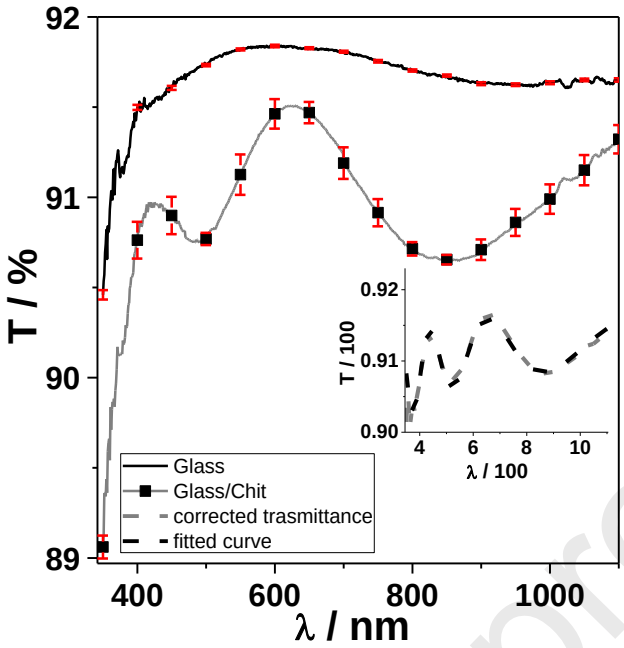

Figure 2s: Transmittance spectra of glass and chitosan-coated glass, fitted curve to determine layer thickness and refractive index (inset). Experimental conditions: wavelength range 350-1100 nm

Journal Pre-proofs

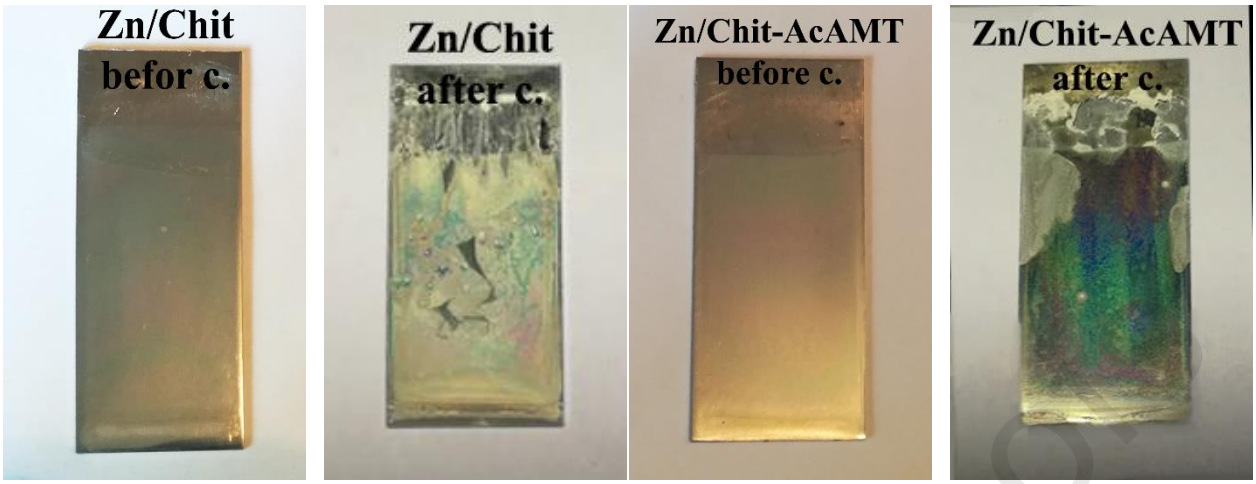

Figure 3s: Visual inspection of Zn/Chit and Zn/Chit-AcAMT samples before and after 3 days of exposure to 0.2 g/L Na_2SO_4 solution

The color observed in the case of the coated samples is due to thin layer interference phenomenon.

Journal Pre-proofs

Highlights

- Zn substrates were coated with thin layers of chitosan
- 2-Acetylamino-5-mercapto-1,3,4-thiadiazole (AcAMT) was accumulated in the coating
- Anticorrosive protection efficiency of the system was verified by multiple methods
- The Chit-AcAMT coating provides good protection with >90% inhibition efficiency
- Chit-AcAMT is an eco-friendly, low cost choice in the temporary protection of Zn

Journal Pre-proofs

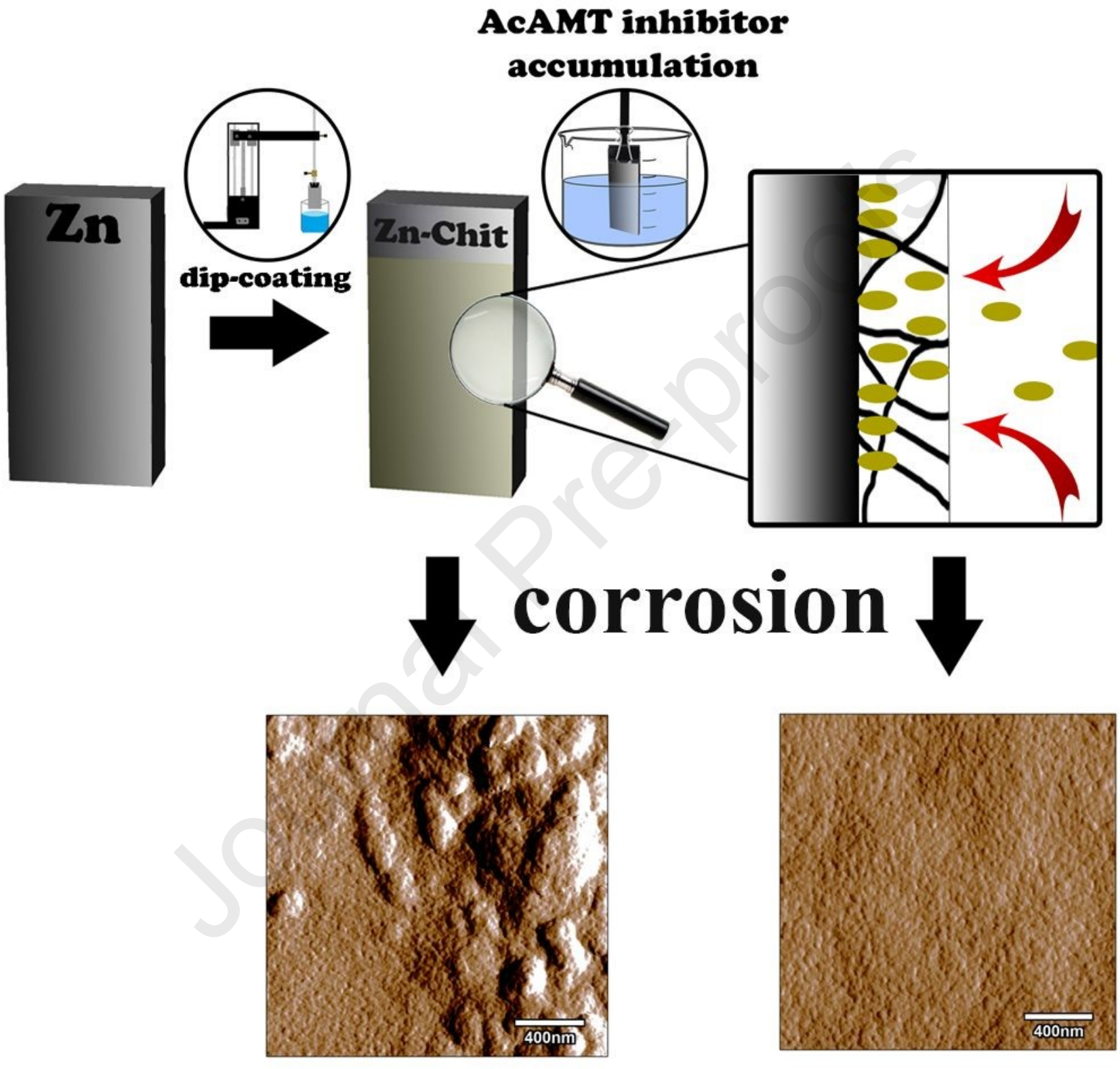

Journal Pre-proofs